Chemical Science

Accepted Manuscript

This article can be cited before page numbers have been issued, to do this please use: H. Chen, W. Lin, Z. Zhang, Z. Yang, K. Jie, J. Fu, S. Yang and S. Dai, *Chem. Sci.*, 2020, DOI: 10.1039/D0SC02238A.

ROYAL SOCIETY OF CHEMISTRY

rsc.li/chemical-science

View Article Online
DOI: 10.1039/D0SC02238A

MMUNICATION

Facile Benzene Reduction Promoted by A Synergistically Coupled Cu-Co-Ce Ternary Mixed Oxide

Received 00th January 20xx,
Accepted 00th January 20xx

DOI: 10.1039/x0xx00000x

Hao Chen[a,b †], Wenwen Lin[a †], Zihao Zhang[a †], Zhenzhen Yang[b], Kecheng Jie[b], Jie Fu[a*], Shi-ze Yang[d*], Sheng Dai[b,c*]

Hydrogenation of aromatic ring promoted by earth-abundant metal composites under mild conditions is a long term attractive and challenging subject. In this work, a simple active site creation and stabilization strategy was employed to obtain Cu^+-containing ternary mixed oxide catalyst. Simply by pre-treatment of the ternary metal oxide precursor under H_2 atmosphere, a Cu^+-derived heterogeneous catalyst was obtained and denoted as $Cu_1Co_5Ce_5O_x$. The catalyst was featured by (1) high Cu^+ species content, (2) uniform distribution of Cu^+ doped in the lattices of CoO_x and CeO_2, (3) formation of CoO_x/CuO_x and CeO_2/CuO_x interfaces, and (4) mesoprous structure. These unique properties of $Cu_1Co_5Ce_5O_x$ render it pretty high hydrogenation activity of aromatic rings under mild conditions (100 °C with 5 bar of H_2), which is much higher than the corresponding binary conterparts and even exceeds the performance of the commercial noble metal catalysts (e.g. Pd/C). Synergetic effect plays a crucial role in the catalytic procedure with CeO_2 functioning as hydrogen dissociation and transfer media, Cu^+ hydrogenating the benzene ring and CoO_x stabilzing the unstable Cu^+ species. This will unlock new opportunity to design highly efficient earth-abundant metal-derived heterogeneous catalysts via interface interaction.

Hydrogenation is among the central themes of petrochemical, coal chemical, fine chemical and environmental industries and is one of the most intensively investigated topics in catalysis. [1-4] In addition, in the synthesis of fine chemicals, reduction of various functional groups, such as -C=C, -C≡C, -C=O, -NO_2, -C≡N, -COOH, and -$CONH_2$, are required to afford the corresponding alkanes, alkenes, alcohols, and amine products that are key intermediates for the fine chemical, polymer, agrochemical, and pharmaceutical industries, especially using H_2 as a clean and cheap hydrogen source. [5, 6] Among all these transformations, hydrogenation of benzene is a direct and important approach to afford cycloalkane intermediates for petrochemical and agrochemical productions, and has received enormous attention during the past few decades.[7-9] However, the π-conjugation in aromatic rings makes it one of the most robust chemical bonds due to high aromaticity and non-polarity.[10-12] Over the past decades, technologies mainly depending on expensive and precious metals-based catalysts, such as Pd, Ru, Pt, and Ir, have been extensively investigated to facilitate this transformation. Concerns on the scarcity and high cost of noble metals have driven the search for nonprecious earth-abundant alternatives with comparable activity, selectivity and stability, which are greatly desired for scalable and cost-effective chemical transformations.[11-18] To date, there have been a few reports on Ni/Al_2O_3 , Ni/SiO_2, Co/SiO_2 and Ni-Al alloys that can partially or fully hydrogenate benzene with transition metal-based catalysts, but harsh reaction conditions (e.g. high reaction temperature up to 200 °C and high H_2 pressure up to 8 MPa) and low weight hourly space velocity (WHSV) limit their further application. [19-21] Therefore, despite intensive studies on the subject of benzene hydrogenation, catalytic systems based on nonprecious metals capable of promoting the reaction under mild conditions are still rarely reported. Significant challenges are still existed to develop a cheap, easily synthesized and highly efficient heterogeneous catalysts derived from earth-abundant alternatives by rational design.

In this aspect, we focus our attention on one of the most challenging kind of metal species based on copper, which is pretty cheap and abundant. On the other hand, copper-based catalysts have been widely investigated for the hydrogenation of biomass[22, 23] and CO_2,[24-27] with the activity being mainly attributed to the Cu^0 species in vapor-phase reactions.[23, 28] For instance, Ma et al. revealed that the formation rate of alcohol is strongly correlated with the density of surface Cu^0 sites.[25, 29] Notably, compared with Cu^0 and Cu^{2+}, Cu^+ has a higher hydrogenation activity considering its intrinsic ability to facilitate electron transfer through gaining or losing electron.[25, 30, 31] Many studies have reported that Cu^0/Cu^+ leads to an enhanced catalytic activity for hydrogenation, which is attributed to the activation of the ester groups by Cu^+ species in the production of alcohols.[30, 32-34] However, these conjectures are inconclusive as Cu^+ is synthetically challenging due to the tendency to become easily oxidized to Cu^{2+} or reduced to Cu^0 during catalyst preparation and processing. Key to success lies in the design and fabrication of copper-involved composites capable of stabilizing the highly active Cu^+ species through interface interactions. This will also bring a deeper understanding of the catalytic contributions from the Cu^+ species, which is significant for the rational design of active hydrogenation catalysts.

[a] Key Laboratory of Biomass Chemical Engineering of Ministry of Education, College of Chemical and Biological Engineering, Zhejiang University, Hangzhou 310027, China
[b] Department of Chemistry, University of Tennessee, Knoxville, TN 37996, United States
[c] Chemical Sciences Division, Oak Ridge National Laboratory, Oak Ridge, TN 37831, United States
[d] Eyring Materials Center, Arizona State University, Tempe, United States 85257‡
†These authors contributed equally.

Electronic Supplementary Information (ESI) available: [details of any supplementary information available should be included here]. See DOI: 10.1039/x0xx00000x

View Article Online
DOI: 10.1039/D0SC02238A

As previously reported, CoO_y in Cu catalyst not only enhances the metallic Cu dispersion and H_2 activation ability, but also modifies the chemical states of Cu to create proper surface Cu^0/Cu^+ distributions due to strong electronic interaction at the Cu/CoO_x interface.[35] This inspires us to fabricate multi-component heterogenous catalysts involving Cu^+ species. It is known that the adsorption and activation of H_2 constitutes another critical step in the hydrogenation reactions. Various kinds of materials have been reported to activate H_2 by homolytic or heterolytic dissociation. [36, 37] Recently, Sai et al. created a solid frustrated Lewis pairs (FLPs) on the surface of CeO_2 by regulating their surface defects. The resultant catalysts exhibited H_2 dissociation ability with a low activation barrier and delivered a high catalytic activity for hydrogenation of alkenes and alkynes, as well as transformation of CO_2[38, 39]. However, the catalytic activity of these CeO_2-based materials is still insufficient to achieve hydrogenation of aromatic rings. Therefore, we envisage that the combination of Cu, Co and Ce species would create enhanced H_2 activation capability, realize the hydrogenation of aromatic rings under mild conditions by synergistic effect, and lead to further understanding of the interface interaction during the catalytic procedure.

The previous studies in our group has developed a simple fabrication procedure of ternary CuO–Co_3O_4–CeO_2 catalyst, which showed excellent catalytic activity on CO oxidation [40]. Herein, a simple active site creation and stabilization strategy was employed to obtain Cu^+-containing ternary mixed oxide catalyst. Simply by pre-treatment of the ternary metal oxide precursor under H_2 atmosphere, a Cu^+-derived heterogeneous catalyst was obtained and denoted as $Cu_1Co_5Ce_5O_x$. The catalyst was featured by (1) high Cu^+ species content, (2) uniform distribution of Cu^+ doped in the lattices of CoO_x and CeO_2, (3) formation of CoO_y/CuO_x and CeO_2/CuO_x interfaces, and (4) mesoprous structure. These unique properties of $Cu_1Co_5Ce_5O_x$ render it pretty high hydrogenation activity of aromatic rings under mild conditions (100 °C with 5 bar of H_2), which is much higher than the corresponding binary counterparts and even exceeds the performance of the commercial noble metal catalysts (e.g. Pd/C). Synergetic effect plays a crucial role in the catalytic procedure with CeO_2 functioning as hydrogen dissociation and transfer media, Cu^+ hydrogenating the benzene ring and CoO_x stabilzing the unstable Cu^+ species. This will unlock new opportunity to design highly efficient earth-abundant metal-derived heterogeneous catalysts via interface interaction.

The ternary $Cu_1Co_5Ce_5O_x$ catalyst was prepared via a two-step approach involving co-precipitation and heat-treatment. $Cu_1Co_5Ce_5O_y$ with Cu: Co: Ce atomic ratios of 1: 5: 5 was first synthesized using a co-precipitation method[40, 41] and further pre-treatment at 100 °C with 5 bar of H_2 for 24 h leads to the formation of $Cu_1Co_5Ce_5O_x$. The ICP result as shown in Table S1 confirmed the Cu: Co: Ce atomic ratio was almost the same as the calculated by raw ratio. The XRD pattern of $Cu_1Co_5Ce_5O_y$ in Figure 1a suggests that the as-synthesized ternary oxides are composed of crystalline CeO_2 and Co_3O_4. After H_2 heat-treatment, no change for the diffraction peaks of CeO_2 and Co_3O_4 was found in $Cu_1Co_5Ce_5O_x$. Then, we compared the XRD of CeO_2 (PDF#81-0792) [42], Co_3O_4 (PDF-74-1657) [43] and $Cu_1Co_5Ce_5O_x$ as shown in Figure 1 (a) to further prove that the Cu is doped into the lattices of CoO_y and CeO_2 for $Cu_1Co_5Ce_5O_x$. It was found that the XRD peaks for Ce and Co in $Cu_1Co_5Ce_5O_x$ shifted lower 2 theta angle, which mean the larger lattice parameter of the CeO_2 and Co_3O_4 in $Cu_1Co_5Ce_5O_x$ than the pure CeO_2 and Co_3O_4 after the introduction of copper species and provided the evidence that the Cu ions are incorporated into the CeO_2 and Co_3O_4 crystallites in $Cu_1Co_5Ce_5O_x$ [42, 44].Then we investigated the structure of $CuCoO_x$ (Cu: Co=1: 10 mole ratio), $CuCeO_x$ (Cu: Ce=1: 10 mole ratio) and $CoCeO_x$ (Ce: Co=1: 1 mole ratio) by the XRD and the results are shown in Figure S1. The results showed that the 10 mol% Cu dispersed well in the CoO_x and CeO_x with almost no Cu XRD peak appeared. Thus, in this work, the Cu uniformly distributed among CoO_y and CeO_2, respectively. XPS was performed to probe the oxidation states of Co and Cu on the surface of the ternary oxides. As shown in Figure 1 b-d, both Cu 2p and Co 2p peaks exhibit peak shifts towards lower energies, indicating the H_2 pre-treatment significantly reduces the surface of $Cu_1Co_5Ce_5O_y$ and partially lower the oxidation states of the metal species (Cu^{2+} 934.1 eV, Co^{3+} 781.2 eV, Cu^+/Cu^0 932.0 eV and Co^{2+} 779.2 eV, Table S2).[45] Considering the overlap of the XPS peaks corresponding to Cu^+ and Cu^0, we turned to Cu LMM to determine the Cu oxidation states in the ternary oxide catalysts (Figure 1d and Figure S2), where only Cu^{2+} (569.3 eV) was observed in the $Cu_1Co_5Ce_5O_y$ catalyst while only Cu^+ (573.2 eV) was observed in the $Cu_1Co_5Ce_5O_x$ catalyst.[46-48] Therefore, spectroscopic results indicate that Cu^+ and Co^{2+} are formed on the surface of $Cu_1Co_5Ce_5O_x$ after the H_2 pre-treatment. CeO_2 exhibits hydrogenation activity for unsaturated compounds as the oxidation states of Ce can change

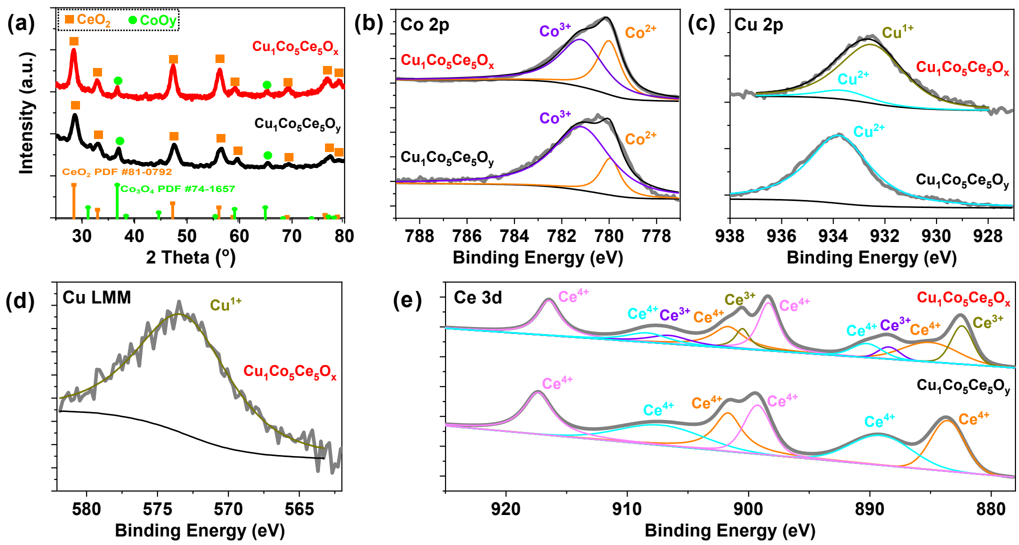

Figure 1. (a) XRD patterns, (b) XPS results of Co 2p, (c) Cu 2p, (d) Cu-LMM, and (e) Ce 3d in $Cu_1Co_5Ce_5O_y$ and $Cu_1Co_5Ce_5O_x$ obtained before and after pre-treatment under the 5 bar H_2 and 100 °C temperature for 24 h.

View Article Online
DOI: 10.1039/D0SC02238A

MMUNICATION

reversibly between Ce^{4+} under oxidizing conditions and Ce^{3+} under reducing conditions.[49, 50] As shown in Figure 1e, XPS have been investigated for $Cu_1Co_5Ce_5O_y$ and $Cu_1Co_5Ce_5O_x$ to distinguish between the Ce^{4+} and Ce^{3+} species, where the peaks shifted to lower binding energy may be due to a higher proportion of Ce^{3+} [50]. Chen et al[51] reported that the active Cu clusters consist of Cu^0 at the top layer and Cu^+ species at the Cu/CeO_2 interface due to electron depletion caused by the oxygen vacancies (O_v) in CeO_2. In our case, the H_2 pre-treatment may create more oxygen vacancies which stabilize Cu^+ through forming the Cu^+–O_v–Ce^{3+} interfacial bonds. It was found that the Cu species in $CuCoCeO_y$ after pre-treatment of 6 h and 18 h were almost maintained at Cu^{2+} state (Figure S3). However, it seemed that the Co was easily to be reduced and more Co^{2+} was formed compared with the $CuCoCeO_y$ after pre-treatment of 6 h and 18 h. And for Ce, the Ce in $CuCoCeO_y$ after pre-treatment of 6 h did not change any more compared with all Ce in $CuCoCeO_y$ was Ce^{4+}, and a little amount of Ce^{3+} was formed after pre-treatment of 18 h.

As reported in our previous work,[40, 41] the as-synthesized $Cu_1Co_5Ce_5O_y$ without H_2 treatment showed a structure of copper–ceria and cobalt–ceria interface (Figure S4). To further probe the structural details of the ternary $Cu_1Co_5Ce_5O_x$ as well as the interface of $CoO_y(Cu_2O)$–$CeO_2(Cu_2O)$, STEM–HAADF with EDS element mapping was conducted as shown in Figure 2. The absence of the diffraction peaks corresponding to Cu, Cu_2O, or CuO in the XRD pattern (Figure 1a), together with a uniform distribution of Cu among CoO_y and CeO_2 in the STEM-EDS element maps (Figure 2), suggests that Cu is doped into the lattices of CoO_y and CeO_2 for $Cu_1Co_5Ce_5O_x$ and form CoO_y/CuO_x and CeO_2/CuO_x interfaces.

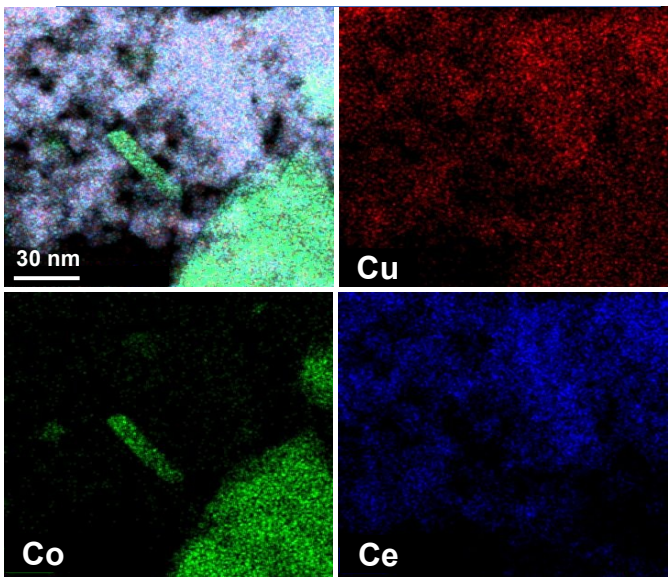

Figure 2. STEM–HAADF images and EDS elements mapping of Cu, Co and Ce in Cu1Co5Ce5Ox catalyst.

The N_2 adsorption–desorption isotherm at 77 K is shown in Figure 3a and the sample exhibits typical IV shape isotherm, suggesting the existence of mesopores with 2-10 nm pore diameters in $Cu_1Co_5Ce_5O_x$ after H_2 treatment. The Brunauer–Emmett–Teller (BET) surface area of the $Cu_1Co_5Ce_5O_x$ is estimated to be 82 m^2 g^{-1} with a total pore volume of 0.13 m^3 g^{-1} (Figure 3), which is a little higher compared with the $Cu_1Co_5Ce_5O_y$ before H_2 treatment (78 m^2 g^{-1}). Notably, mesopores played a dominant role in the pore structure, contributing ~99% of the total pore volume (V_{micro}=0 m^3 g^{-1}, calculated using the t-plot method). For catalytic or adsorptive materials, a high surface area together with mesoporous structure can dramatically enhance their reactivity due to an improved mass transfer effect.[52, 53]

Acetyl benzene is selected as a model substrate to evaluate the catalytic property of $Cu_1Co_5Ce_5O_x$ (Figures 4a). In a typical catalytic experiment, 100 mg of $Cu_1Co_5Ce_5O_y$ was pre-treated at 100 °C with 5 bar of H_2 for 24 h. Then 150 mg acetyl benzene (A) and 5 ml hexane was added to the reaction solution for hydrogenation under the same condition. The H_2-pretreated ternary oxide catalyst $Cu_1Co_5Ce_5O_x$ exhibits excellent activity towards complete hydrogenation of both acetyl and benzene groups, producing ethylcyclohexane (D) with 100 % conversion and 97 % yield, which even exceeds the performance of the commercial 5 wt% Pd/C catalysts (74% conversion and 72% yield) under the same reaction condition (Figure 4b). Further control experiments show that the

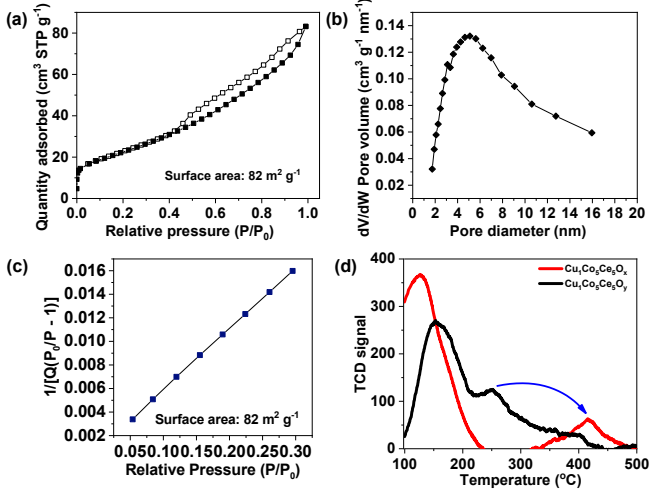

Figure 3. (a) N_2 adsorption/desorption isotherm at 77 K, (b) pore size distribution curve, (c) BET plot, and (d) Benzene temperature program desorption of $Cu_1Co_5Ce_5O_x$ catalysts.

untreated ternary oxide catalyst $Cu_1Co_5Ce_5O_y$ exhibited much inferior hydrogenation capability, with ethylbenzene (C) being obtained as the sole product (Figure S5). To further investigate the synergetic effect of the ternary oxides, the H_2-pretreated binary oxide catalysts including $CuCeO_x$, $CuCoO_x$, and $CoCeO_x$ were prepared and the catalytic results indicated that ethylbenzene (C) was obtained in the presence of $CuCeO_x$ and $CuCoO_x$, and using $CoCeO_x$ as the catalyst, only reduction of carbonyl group can be achieved, affording 1-phenylethanol as the product. That is, none of them showed the ability to hydrogenate benzene ring. In addition, selective hydrogenation was realized using catalysts obtained by pre-treating $Cu_1Co_5Ce_5O_y$ under hydrogen with different times. Then, the XPS of the $CuCoO_x$ and $CuCeO_x$ were measured (Figure S6). It can be found that without synergistic effect of CoO_x and CeO_x, the Cu species in $CuCoO_x$ and $CuCeO_x$ after H_2 pre-treatment all existed as Cu^{2+} and Cu^0, and controlled reduction to Cu^+ cannot be achieved.

This was also proved by the CODRIFTs as shown in the Figure S7. Therefore, Cu^+ was the key factor in this work to achieve successful hydrogenation of benzene ring. The generated $Cu_1Co_5Ce_5O_x$ catalysts exhibited distinct hydrogenation capabilities. As summarized in Figure 4c, H_2-pretreatments with 6 h, 18 h, and 24 h lead to the formation of 96 % of ethyl benzene (C), 98 % of ethyl benzene (C), and 97 % of ethyl-cyclohexane (D), respectively. Therefore, the H_2-pretreated ternary Cu-Co-Ce oxides shows an excellent capability towards the hydrogenation of aromatic rings.

As previously reported, compared with Cu^0 and Cu^{2+}, Cu^+ has a higher hydrogenation activity considering its intrinsic ability to facilitate electron transfer through gaining or losing electron.[25, 30, 31] Many studies have reported that Cu^0/Cu^+ leads to an enhanced catalytic activity for hydrogenation, which is attributed to the activation of the ester groups by Cu^+ species.[30, 33, 34] However, it is difficult to isolate Cu^+ species for direct comparison, as it can rapidly convert to Cu^0 or Cu^{2+} during catalyst preparation and processing. Here we report a ternary oxide system $Cu_1Co_5Ce_5O_x$ where Cu^+ can be formed and stabilized through a simple pretreatment under H_2. As previously reported, CoO_y in Cu catalyst not only enhances the metallic Cu dispersion and H_2 activation ability, but also modifies the chemical states of Cu to create proper surface Cu^0/Cu^+ distributions due to strong electronic interaction at the Cu/CoO_x interface.[35] In our case, Cu is doped into the lattices of CoO_y and CeO_2 for $Cu_1Co_5Ce_5O_x$ and CoO_y exists as a promotor to stabilize Cu^+ under 5 bar H_2 and 100 °C through interfacial effects with CeO_2. This is further supported by the emergence of Cu^0 after the pretreatment of $CuCeO_x$ (Figures S6~S7), indicating that Cu^{2+} will be reduced to Cu^0 without cobalt. The stabilized Cu^+ in $Cu_1Co_5Ce_5O_x$ exhibits an excellent catalytic performance for the hydrogenation of both benzene and C=O, whereas $CuCeO_x$, $CuCoO_x$, and $CoCeO_x$ exhibit limited conversion and selectivity of converting acetyl benzene to ethylcyclohexane. It was also reported that the defect-enriched CeO_2 constructed interfacial frustrated Lewis pairs ($Ce^{3+}\cdots O^{2-}$) that effectively activate the H_2 and CO_2 [38, 39] and XPS results show that the H_2 pretreatment lead to the formation of Ce^{3+} with oxygen vacancy on the surface. Chen et al[51]

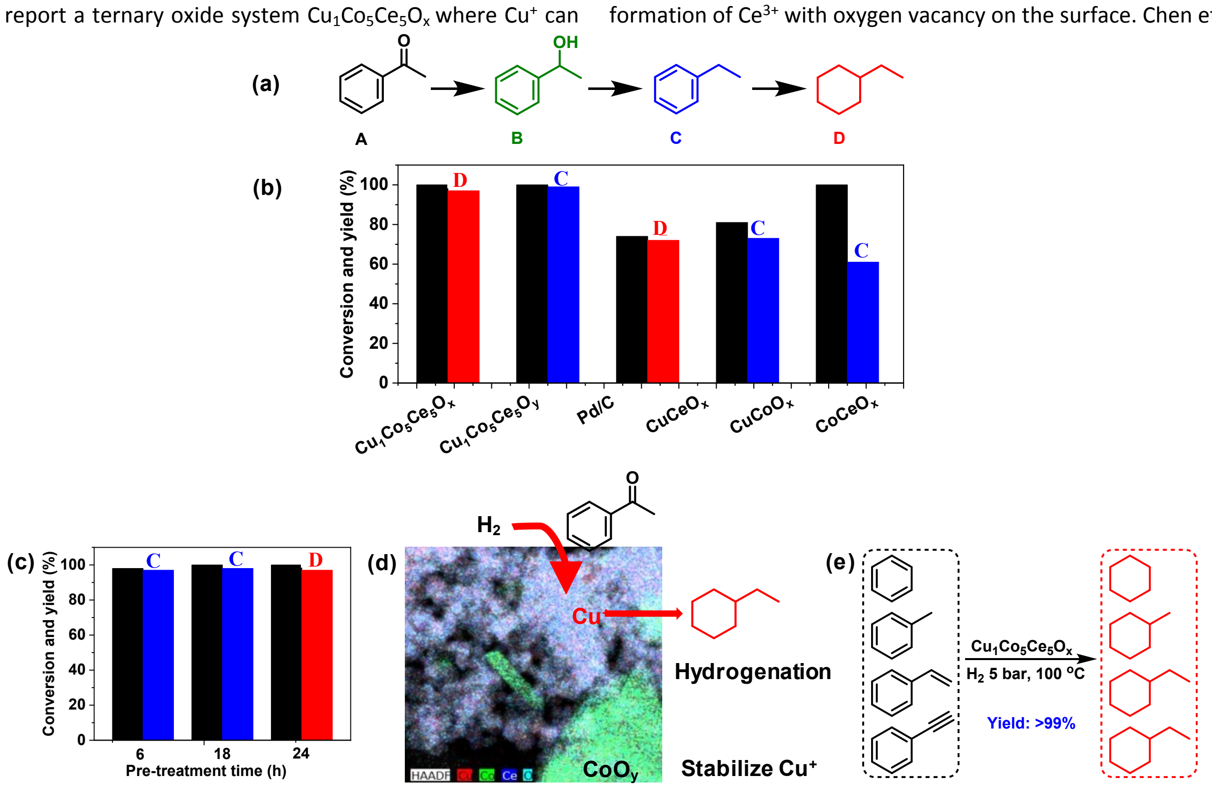

Figure 4. (a) Catalytic hydrodeoxygenation of acetyl benzene. (b) Comparison of the catalytic activity using $Cu_1Co_5Ce_5O_x$, $Cu_1Co_5Ce_5O_y$, Pd/C and $CuOCeO_2$, CoO_yCeO_2, $CuOCoO_y$ after H_2 pretreatment. (c) Catalytic hydrodeoxygenation of acetyl benzene over $Cu_1Co_5Ce_5O_y$ catalyst with different pre-treatment times. (d) Synergistic effect of Cu_2O, CoO_y and CeO_2 in the CCC catalyst. (e) Hydrogenation of other aromatic compounds containing benzene ring. All the reaction was performed under the following conditions: catalyst (100 mg), hexane (5 mL), substrate (1.25 mmol), reaction time (24 h), temperature (100 °C), H_2 (5 bar). Acetyl benzene was used as the substrate for the results in (a) and (b).

also reported that the Cu^+ species directly bonded to the oxygen vacancy in CeO_2 exhibits a high activity for the water–gas shift reaction, where Cu^+ site chemically adsorbs CO whereas the neighbouring O_v–Ce^{3+} site activates H_2O. Thus, CeO_2 functions as hydrogen dissociation and transfer media by the $Ce^{3+}\cdots O^{2-}$ frustrated Lewis pairs [54] and then the neighbouring Cu^+ hydrogenated the benzene as shown in the Figure 4d. In addition, benzene temperature program desorption (Ben–TPD) were performed to study the adsorption capacity of benzene ring on $Cu_1Co_5Ce_5O_y$ and $Cu_1Co_5Ce_5O_x$ catalyst as shown in Figure 3d. The observed two peaks at 100~200 and 250~450 °C are attributed to physical and chemical adsorption of benzene on the two oxide catalysts, respectively. Clearly, chemisorption of benzene on $Cu_1Co_5Ce_5O_y$ is enhanced after H_2 pretreatment as evidenced by the desorption temperature being increased from 250 °C to 420 °C, probably due to the strong interaction between benzene and a withdrawing Cu^+ from the oxygen ring.[55] Besides acetyl benzene, a series of benzene and benzene derivatives including benzene, phenylacetylene and methylbenzene, are also fully hydrogenated to the corresponding alkanes using the $Cu_1Co_5Ce_5O_x$ catalyst under mild conditions (Figure 4e), demonstrating the wide applicability of the ternary oxides for efficient benzene hydrogenation. In summary, a new type of Cu-Co-Ce ternary mixed oxide catalyst with remarkable hydrogenation activity of benzene is reported. Formation of Cu^+ during a simple pretreatment process is considered to be the key of the activity promotion, while CoO_x function as the Cu^+ stabilizer and CeO_2

facilitates the dissociation and transfer of hydrogen. Demonstration of Cu^+ in $Cu_1Co_5Ce_5O_x$ as the key component leading to extraordinary hydrogenation activity of substituted benzenes, provides new insights into the design and modification of noble-metal-free catalysts for a wide scope of heterogeneous transformations. The resultant turnover number (TON) using $Cu_1Co_5Ce_5O_y$, $Cu_1Co_5Ce_5O_x$ and commercial 5wt% Pd/C in this work was compared. The TON obtained in different catalytic systems was estimated based on the following equation: TON = mmol (ethylbenzene)/mmol (active site)][56, 57]. As a result, the TON of the $Cu_1Co_5Ce_5O_y$, $Cu_1Co_5Ce_5O_x$ and commercial 5wt% Pd/C was calculated to be 0, 38.8 and 18.6. It was found that the $Cu_1Co_5Ce_5O_x$ obtained after H_2 pre-treatment exhibited a TON value double that obtained using Pd/C catalyst. At last, the results of stability in reuses (five times) as well as the XPS and XRD measurements are shown in Figures S8~S10. It was found that the Cu^+ remained the 1^+ valance after the hydrogenation (Figure S8). This is because that the catalyst was pre-treated in the same condition as the reaction condition. Thus, during the reaction process within 24 h, the catalyst was stable and there should be no change of valence state during the catalytic recycling (Figure S10). The catalytic results showed that the catalyst showed very good reusability for at least five times without any decrease in the catalytic activity, with >99% conversion of acetyl benzene with >95% yield of ethylcyclohexane being obtained in the fifth run. And the XRD results showed that the structure of the recycled catalyst maintained well after catalyzing the hydrogenation reaction.

Conflicts of interest

There are no conflicts to declare.

Acknowledgements

This work was supported by the U.S. Department of Energy, Office of Science, Office of Basic Energy Sciences, Chemical Sciences, Geosciences, and Biosciences Division. J. F. was supported by the National Natural Science Foundation of China (No. 21978259, 21706228) and the Zhejiang Provincial Natural Science Foundation of China (No. LR17B060002). The STEM used resources of the Center for Functional Na-nomaterials, which is a U.S. DOE Office of Science Facility, at Brookhaven National Laboratory under Contract No. DE-SC0012704.

Notes and references

1. R. A. Johnstone, A. H. Wilby and I. D. Entwistle, *Chem Rev*, 1985, **85**, 129-170.
2. F. Meemken and A. Baiker, *Chem Rev*, 2017, **117**, 11522-11569.
3. D. Wang and D. Astruc, *Chem Rev*, 2015, **115**, 6621-6686.
4. L. Zhang, M. Zhou, A. Wang and T. Zhang, *Chem Rev*, 2019.
5. L. Alig, M. Fritz and S. Schneider, *Chem Rev*, 2018, **119**, 2681-2751.
6. W. Wang, S. Wang, X. Ma and J. Gong, *Chem Soc Rev*, 2011, **40**, 3703-3727.
7. S. Miao, Z. Liu, B. Han, J. Huang, Z. Sun, J. Zhang and T. Jiang, *Angew Chem Int Ed*, 2006, **45**, 266-269.
8. C. P. Rader and H. A. Smith, *J Am Chem Soc*, 1962, **84**, 1443-1449.
9. L. Foppa and J. Dupont, *Chem Soc Rev*, 2015, **44**, 1886-1897.
10. X. Kang, G. Luo, L. Luo, S. Hu, Y. Luo and Z. Hou, *J Am Chem Soc*, 2016, **138**, 11550-11559.
11. H. Liu, R. Fang, Z. Li and Y. Li, *Chem Eng Sci*, 2015, **122**, 350-359.
12. C. Hubert, E. G. Bilé, A. Denicourt-Nowicki and A. Roucoux, *Green Chem*, 2011, **13**, 1766-1771.
13. H. Liu, T. Jiang, B. Han, S. Liang and Y. Zhou, *Science*, 2009, **326**, 1250-1252.
14. P. Zhang, T. Wu, T. Jiang, W. Wang, H. Liu, H. Fan, Z. Zhang and B. Han, *Green Chem*, 2013, **15**, 152-159.
15. K. M. Bratlie, H. Lee, K. Komvopoulos, P. Yang and G. A. Somorjai, *Nano Lett*, 2007, **7**, 3097-3101.
16. C. Vangelis, A. Bouriazos, S. Sotiriou, M. Samorski, B. Gutsche and G. Papadogianakis, *J Catal*, 2010, **274**, 21-28.
17. P. Tomkins, E. Gebauer-Henke, W. Leitner and T. E. Müller, *ACS Catal.*, 2014, **5**, 203-209.
18. J.-F. Yuan, C.-Q. Luo, Q. Yu, A.-P. Jia, G.-S. Hu, J.-Q. Lu and M.-F. Luo, *Catal. Sci. Technol.*, 2016, **6**, 4294-4305.
19. X. Kang, H. Liu, M. Hou, X. Sun, H. Han, T. Jiang, Z. Zhang and B. Han, *Angewandte Chemie International Edition*, 2016, **55**, 1080-1084.
20. R. Molina and G. Poncelet, *J Catal*, 2001, **199**, 162-170.
21. L. Lu, Z. Rong, W. Du, S. Ma and S. Hu, *ChemCatChem*, 2009, **1**, 369-371.
22. Z. Zhang, Q. Yang, H. Chen, K. Chen, X. Lu, O. Pingkai, J. Fu and J. G. Chen, *Green Chem*, 2017, **20**, 197-205.
23. Z. Zhang, S. Yao, C. Wang, M. Liu, F. Zhang, X. Hu, H. Chen, X. Gou, K. Chen, Y. Zhu, X. Lu, P. Ouyang and J. Fu, *J Catal*, 2019, **373**, 314-321.
24. B. An, J. Zhang, K. Cheng, P. Ji, C. Wang and W. Lin, *J Am Chem Soc*, 2017, **139**, 3834-3840.
25. J. Gong, H. Yue, Y. Zhao, S. Zhao, L. Zhao, J. Lv, S. Wang and X. Ma, *J Am Chem Soc*, 2012, **134**, 13922-13925.
26. Z.-Q. Wang, Z.-N. Xu, S.-Y. Peng, M.-J. Zhang, G. Lu, Q.-S. Chen, Y. Chen and G.-C. Guo, *ACS Catal.*, 2015, **5**, 4255-4259.
27. S. Kattel, P. J. Ramírez, J. G. Chen, J. A. Rodriguez and P. Liu, *Science*, 2017, **355**, 1296-1299.
28. R. Reske, H. Mistry, F. Behafarid, B. R. Cuenya and P. Strasser, *J Am Chem Soc*, 2014, **136**, 6978-6986.
29. S. Zhao, H. Yue, Y. Zhao, B. Wang, Y. Geng, J. Lv, S. Wang, J. Gong and X. Ma, *J Catal*, 2013, **297**, 142-150.
30. X. Chang, T. Wang, Z. J. Zhao, P. Yang, J. Greeley, R. Mu, G. Zhang, Z. Gong, Z. Luo, J. Chen, Y. Cui, G. A. Ozin and J. Gong, *Angew Chem Int Ed*, 2018, **57**, 15415-15419.
31. W. Chen, T. Song, J. Tian, P. Wu and X. Li, *Catal. Sci. Technol.*, 2019, **9**, 6749-6759.
32. C. Wen, A. Yin, Y. Cui, X. Yang, W.-L. Dai and K. Fan, *Appl. Catal. A: Gen.*, 2013, **458**, 82-89.
33. Y. Wang, Y. Shen, Y. Zhao, J. Lv, S. Wang and X. Ma, *ACS Catal.*, 2015, **5**, 6200-6208.
34. S. Zhang, Y. Ma, H. Zhang, X. Zhou, X. Chen and Y. Qu, *Angew Chem Int Ed*, 2017, **56**, 8245-8249.
35. J. Wu, G. Gao, P. Sun, X. Long and F. Li, *Acs Catal.*, 2017, **7**, 7890-7901.
36. D. Teschner, J. Borsodi, A. Wootsch, Z. Révay, M. Hävecker, A. Knop-Gericke, S. D. Jackson and R. Schlögl, *Science*, 2008, **320**, 86-89.
37. T. Mitsudome, Y. Mikami, M. Matoba, T. Mizugaki, K. Jitsukawa and K. Kaneda, *Angew Chem Int Ed*, 2012, **51**, 136-139.
38. S. Zhang, Z. Xia, Y. Zou, F. Cao, Y. Liu, Y. Ma and Y. Qu, *J Am Chem Soc*, 2019, DOI: 10.1021/jacs.9b03217.
39. S. Zhang, Z. Q. Huang, Y. Ma, W. Gao, J. Li, F. Cao, L. Li, C. R. Chang and Y. Qu, *Nat. Commun.*, 2017, **8**, 15266.
40. A. J. Binder, T. J. Toops, R. R. Unocic, J. E. Parks and S. Dai, *Angew Chem Int Ed*, 2015, **54**, 13263-13267.

View Article Online
DOI: 10.1039/D0SC02238A

41. W. Xiao, S. Yang, P. Zhang, P. Li, P. Wu, M. Li, N. Chen, K. Jie, C. Huang, N. Zhang and S. Dai, *Chem Mater*, 2018, **30**, 2924-2929.
42. C. He, Y. Yu, L. Yue, N. Qiao, J. Li, Q. Shen, W. Yu, J. Chen and Z. Hao, *Applied Catalysis B: Environmental*, 2014, **147**, 156-166.
43. Y. Tak and K. Yong, *The Journal of Physical Chemistry C*, 2008, **112**, 74-79.
44. N. R. Radwan, M. Mokhtar and G. A. El-Shobaky, *Applied Catalysis A: General*, 2003, **241**, 77-90.
45. H. Yan, H. Qin, W. Liang, X. Jin, Y. Zhang, X. Feng, Y. Liu, X. Chen and C. Yang, *Catal. Sci. Technol.*, 2019, **9**, 4909-4919.
46. Y. Tanaka, R. Kikuchi, T. Takeguchi and K. Eguchi, *Appl. Catal. B: Environ.*, 2005, **57**, 211-222.
47. S. Zhu, X. Gao, Y. Zhu, W. Fan, J. Wang and Y. Li, *Catal. Sci. Technol.*, 2015, **5**, 1169-1180.
48. C. Yang, Z. Miao, F. Zhang, L. Li, Y. Liu, A. Wang and T. Zhang, *Green Chem*, 2018, **20**, 2142-2150.
49. L. Vivier and D. Duprez, *ChemSusChem*, 2010, **3**, 654-678.
50. D. Mullins, S. Overbury and D. Huntley, *Surf Sci*, 1998, **409**, 307-319.
51. A. Chen, X. Yu, Y. Zhou, S. Miao, Y. Li, S. Kuld, J. Sehested, J. Liu, T. Aoki and S. Hong, *Nat. Catal.*, 2019, **2**, 334.
52. H. Chen, Q. Wang, X. Zhang and L. Wang, *Appl. Catal. B: Environ.*, 2015, **166-167**, 327-334.
53. H. Chen, Q. Wang, X. Zhang and L. Wang, *Ind Eng Chem Res*, 2014, **53**, 19916-19924.
54. M. García-Melchor and N. López, *J Phys Chem C*, 2014, **118**, 10921-10926.
55. E. Kukulska-Zając, P. Kozyra and J. Datka, *Appl. Catal. A: Gen.*, 2006, **307**, 46-50.
56. A. Dubey, L. Nencini, R. R. Fayzullin, C. Nervi and J. R. Khusnutdinova, *ACS Catalysis*, 2017, **7**, 3864-3868.
57. X. Shao, X. Yang, J. Xu, S. Liu, S. Miao, X. Liu, X. Su, H. Duan, Y. Huang and T. Zhang, *Chem*, 2019, **5**, 693-705.

View Article Online
DOI: 10.1039/D0SC02238A

TOC